JACS
JOURNAL OF THE AMERICAN CHEMICAL SOCIETY

Article

pubs.acs.org/JACS

Insights into the Proton Transfer Mechanism of a Bilin Reductase PcyA Following Neutron Crystallography

Masaki Unno,*[,†,‡] Kumiko Ishikawa-Suto,[†,‡,§] Katsuhiro Kusaka,[†] Taro Tamada,[§] Yoshinori Hagiwara,[∥,⊥] Masakazu Sugishima,[#] Kei Wada,[▽] Taro Yamada,[†] Katsuaki Tomoyori,[†,§] Takaaki Hosoya,[†,‡] Ichiro Tanaka,[†,‡] Nobuo Niimura,[†] Ryota Kuroki,[§] Koji Inaka,[○] Makiko Ishihara,[†] and Keiichi Fukuyama[∥,◆]

[†]Frontier Research Center for Applied Atomic Sciences, Ibaraki University, Naka 319-1106, Japan
[‡]Graduate School of Science and Engineering, Ibaraki University, Hitachi 316-8511, Japan
[§]Quantum Beam Science Center, Japan Atomic Energy Agency, Naka 319-1195, Japan
[∥]Graduate School of Science, Osaka University, Toyonaka 560-0043, Japan
[⊥]Department of Biochemistry and Applied Chemistry, National Institute of Technology, Kurume College, Kurume 830-8555, Japan
[#]Department of Medical Biochemistry, Kurume University School of Medicine, Kurume 830-0011, Japan
[▽]Organization for Promotion of Tenure Track, University of Miyazaki, Kiyotake 889-1692, Japan
[○]MARUWA Foods and Biosciences Inc., Yamatokoriyama 639-1123, Japan
[◆]Graduate School of Engineering, Osaka University, Suita 565-0871, Japan

Supporting Information

ABSTRACT: Phycocyanobilin, a light-harvesting and photoreceptor pigment in higher plants, algae, and cyanobacteria, is synthesized from biliverdin IXα (BV) by phycocyanobilin:ferredoxin oxidoreductase (PcyA) via two steps of two-proton-coupled two-electron reduction. We determined the neutron structure of PcyA from cyanobacteria complexed with BV, revealing the exact location of the hydrogen atoms involved in catalysis. Notably, approximately half of the BV bound to PcyA was BVH^+, a state in which all four pyrrole nitrogen atoms were protonated. The protonation states of BV complemented the protonation of adjacent Asp105. The "axial" water molecule that interacts with the neutral pyrrole nitrogen of the A-ring was identified. His88 Nδ was protonated to form a hydrogen bond with the lactam O atom of the BV A-ring. His88 and His74 were linked by hydrogen bonds via H_3O^+. These results imply that Asp105, His88, and the axial water molecule contribute to proton transfer during PcyA catalysis.

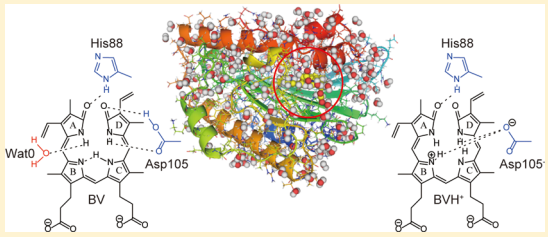

1. INTRODUCTION

Phytobilins are linear tetrapyrroles that perform critical roles in photosynthetic organisms and function as light sensors and light-harvesting antennae.[1−3] Phycocyanobilin (PCB), a phytobilin, comprises the chromophore of algal phytochromes and the core phycobiliprotein antennae of cyanobacteria and red algae. PCB is synthesized by a member of the ferredoxin (Fd)-dependent bilin reductase (FDBR) family, PCB:Fd oxidoreductase (PcyA, EC 1.3.7.5).[4] PcyA is a unique enzyme that catalyzes the reduction of biliverdin IXα (BV) via two sequential steps to produce 3*Z*/3E-PCB (Figure 1). PcyA strictly controls the regiospecificity and reaction sequence of the BV reduction; reduction of the BV D-ring exovinyl group to generate the reaction intermediate, 18^1,18^2-dihydrobiliverdin IXα (18EtBV), precedes A-ring endovinyl reduction.[4] Moreover, PcyA is unique not only because it can catalyze the sequential reduction of two vinyl groups, but also because it is the only enzyme that catalyzes BV D-ring reduction among the FDBRs.[5]

The unique mechanism of BV reduction by PcyA has been studied by structural, biochemical, molecular biological, and theoretical analyses of PcyA from *Synechocystis* sp. PCC 6803 and *Nostoc* sp. PCC 7120.[6−12] From these studies, several unique features of PcyA catalysis have been revealed. First, the existence of two types of positively charged BV (BVH^+) states has been proposed when BV is bound to PcyA.[13,14] One is an N-protonated structure in which four pyrrole N atoms of BV are fully protonated and the bis-lactam state is preserved (Figure 2A).[13] The other is an O-protonated structure in which one or two lactim (C−OH) groups are formed (Figure 2B).[14] Second, electron paramagnetic resonance (EPR) analyses revealed that radical species of the substrate BV were generated

Received: January 24, 2015
Published: April 15, 2015

DOI: 10.1021/jacs.5b00645
J. Am. Chem. Soc. 2015, 137, 5452−5460

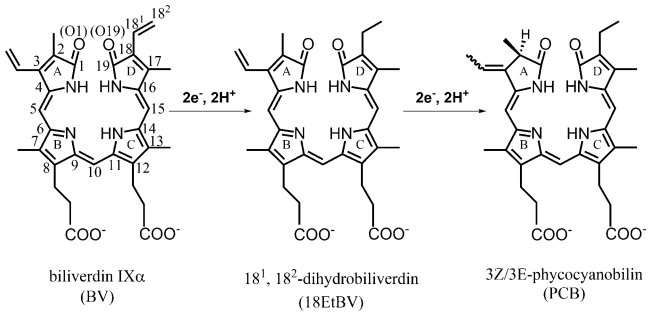

Figure 1. Phycocyanobilin:ferredoxin oxidoreductase (PcyA) reaction. PcyA catalyzes the four-electron reduction of biliverdin IXα (BV) to 3*Z*/3*E*-phycocyanobilin (PCB) via the intermediate 18^1, 18^2-dihydrobiliverdin (18EtBV). Pyrrole rings are labeled A–D.

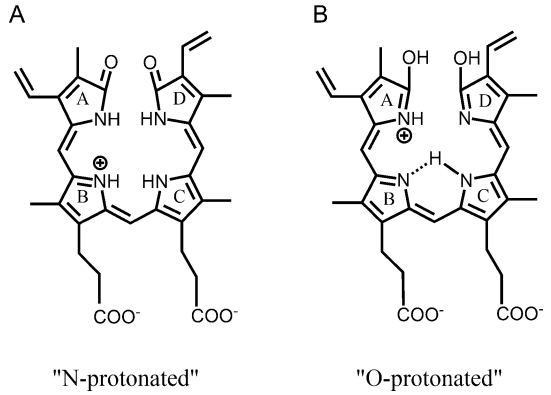

Figure 2. Two types of positively charged BV (BVH^+). (A) N-protonated BVH^+ state. (B) One example of the O-protonated BVH^+ state. O-protonated states can adopt many interconverting tautomers; only one of which is drawn here.

during PcyA catalysis.[12,13] Third, mutational studies and high-resolution X-ray crystal structural studies indicated that His88 and Asp105 (*Synechocystis* numbering) are essential residues, both of which are located near the substrate BV and are thought to be proton donors.[6−8,15] Interestingly, the side chain of Asp105 showed dual conformations in the structures of the PcyA-BV and PcyA-18EtBV complexes.[6,7] Fourth, a structural study of the His88 and Asp105 mutants of PcyA (H88Q and D105N, respectively) identified a water molecule ("axial" water) in the active site, which was ejected upon one-electron reduction.[14] This water molecule was proposed to be essential for catalysis.[14] From these features of PcyA, a proton-coupled electron transfer mechanism including the axial water molecule was proposed for its catalysis.[14] This proposed mechanism, however, has to be reassessed due to two issues. The first issue is the lack of an axial water molecule in the structure of the previous "cryo" wild-type PcyA-BV complex.[7] X-ray structural analyses did not unambiguously confirm the presence of a water molecule at this site. The second issue is the uncertainty of the protonation states of BV, Asp105, and His88 revealed by X-ray crystallography. Knowing the protonation states of the substrate BV and of these essential residues is critical for understanding the catalytic mechanism of the PcyA reaction involving proton transfer.

Although X-ray crystallography is popularly used to study the structure–function relationships of biological macromolecules, it is not the most appropriate method for addressing these issues. One reason for this is that X-rays generate electrons or harmful charged byproducts when they interact with solvent molecules in protein crystals. The charged products can cause enzymatic and/or accidental side reactions and concomitant structural changes, resulting in incorrect structural information in studies of redox enzymes.[16−18] The most important reason is that it is difficult to determine hydrogen atom locations in a protein molecule using X-ray crystallography because X-rays are poorly diffracted by hydrogens.[19] This is especially true in the PcyA structure because some residues, including Asp105, have dual conformations;[7] thus, the occupancies of hydrogens on such residues must be lower, making it much more difficult to determine their locations. Indeed, although we have determined high-resolution X-ray structures of the wild-type and some mutants of the PcyA-BV complex at 1.0 Å resolution, after reporting moderate resolution structures,[6,7] the protonation states of BV and the surrounding residues have not been determined unambiguously. We originally believed that non-charged neutrons do not generate electrons in protein crystals, nor do they alter the active site structure of redox enzymes (however, after the experiment, we realized that this was not exactly true; Supporting Information section 1). Furthermore, in contrast to X-rays, neutrons are strongly diffracted by hydrogen nuclei.[19] Determining the neutron crystal structure of the PcyA-BV complex is the most suitable strategy by which to address the issues mentioned above, that is, the existence of the axial water and the protonation states of BV, Asp105, and His88 in the wild-type PcyA-BV complex. However, neutron crystallography of biological macromolecules also has some disfavored features. First, the neutron fluxes from neutron sources are much smaller than the photon flux of synchrotron X-rays. Thus, much larger crystals are required to obtain a sufficient diffraction image. Second, in neutron diffraction experiments of biological macromolecules, ordinary hydrogen creates a significant background. Therefore, we had to replace the hydrogens in the crystal with deuteriums. In this case, deuterium replaced hydrogen in almost all the O–H and N–H bonds but in almost none of the C–H bonds. The other troublesome point is that the neutron-scattering length for hydrogen also has a negative value; thus, the density maps for hydrogen atoms are negative, whereas those for carbon, nitrogen, sulfur, and deuterium are positive.[19]

In this study, we succeeded in obtaining a very large crystal of the PcyA-BV complex and soaked it into the deuterated solution to exchange the hydrogen atoms in the crystal with deuterium atoms. As a result, neutron diffraction intensity data were able to be collected. We have determined the neutron crystal structure of the PcyA-BV complex at room temperature at 1.95 Å resolution. We observed that approximately half of the BV bound to PcyA was BVH^+, a state in which all four pyrrole nitrogen atoms were protonated (N-protonated), and both of the lactam structures of BV were preserved in wild-type PcyA. The protonation states of the Asp105 dual conformers were clarified, implying the existence of two combinations of BV and Asp105 (BVH^+/deprotonated Asp105 and neutral BV/Asp105). The wild-type PcyA-BV structure, by avoiding X-ray-induced photo reduction, also revealed the existence of the axial water molecule. These results, including hydrogen localizations, will provide crucial information for elucidating the unique catalytic mechanisms of PcyA.

2. EXPERIMENTAL METHODS

2.1. Crystallization of the Wild-Type PcyA-BV Complex for Neutron Crystallography. Expression and purification of wild-type

DOI: 10.1021/jacs.5b00645
J. Am. Chem. Soc. 2015, 137, 5452–5460

Table 1. Statistics for Neutron and X-ray Diffraction Data at Room Temperature

diffraction data collection conditions			
beamline	J-PARC MLF BL03, iBIX		KEK PF-AR, NE3A
wavelength (Å)	3.0−5.6, TOF		1.0
slit size (mm)	5.0 ϕ		0.05 × 0.05
exposure time	9 h/one data set		1 s
transmittance (%)	100		10
sample-to-detector distance (mm)	490.0		150.7
oscillation range (deg)	still		1.0
no. of data sets	24		540 in helical and translational mode
data statistics			
space group	$P2_12_12$		
cell dimensions (Å)	a = 71.0, b = 97.4, c = 43.6		
resolution range (Å) (outer shell)	infinity−1.95 (2.02−1.95)		50.0−1.55 (1.58−1.55)
sources	neutron	neutron (>1σ) (used in the structure refinement)	X-ray
$I/\sigma I$	5.72 (1.48)	6.44 (2.07)	52.8 (6.6)
completeness (%)	93.6 (86.6)	80.7 (57.6)	99.4 (100)
observed reflections	78 063	59 105	673 599
unique reflections	21 333	18 389	43 975
redundancy	3.66	3.21	15.3
R_{sym} [a]	0.164 (0.394)	0.122 (0.200)	0.064 (0.342)

[a] $R_{sym} = \Sigma_{hkl}\Sigma_i|I_i(hkl) - \langle I(hkl)\rangle|/\Sigma_{hkl}\Sigma_i I_i(hkl)$; $\langle I(hkl)\rangle$ is the mean intensity for multiple recorded reflections.

PcyA were conducted as reported previously.[7] The crystallization procedure and conditions were modified from the method reported previously[7] to grow the large crystals necessary for neutron crystallography. Purified PcyA was concentrated to 120 mg/mL by centrifugation using an Amicon Ultra centrifugal (3 kDa) filter unit (Merck Millipore). The PcyA-BV complex was prepared by incubating the concentrated PcyA (550 μL) and BV (4 mM, 615 μL) overnight on ice. The crystal for neutron diffraction was obtained by the sitting drop vapor diffusion method at 293 K from a 20 μL drop of the PcyA-BV complex solution and 20 μL of the reservoir solution containing 200 mM NaCl, 1.4 M ammonium sulfate, and 50 mM MES (pH 5.9). The crystal appeared within 2 weeks. These procedures were performed under dark conditions except for a small green spotlight. The crystal was grown to approximately 2.5 mm × 1.8 mm × 0.6 mm in 1 month (see also Supporting Information section 1).

2.2. Neutron Diffraction Experiment. The crystal was soaked in 50 μL of 50 mM MES buffer (pD 6.3) containing 200 mM NaCl and 1.4 M ammonium-d_8 sulfate (D8, 98%; Cambridge Isotope Laboratories Inc.) prior to neutron diffraction. The soaking solution was exchanged three times in 3 weeks. The soaked crystal was mounted in a quartz glass capillary with 3.5 mm ϕ and 0.01 mm thickness (Hilgenberg) after completing the hydrogen−deuterium exchange. The capillary contained a small amount of deuterated reservoir solution to avoid drying up the crystal, and the capillary was sealed with beeswax and Capillary Wax (Hampton Research). Time-of-flight (TOF) neutron diffraction data were collected at BL03 iBIX[20,21] at the Materials and Life Sciences Experimental Facility (MLF) of the Japan Proton Accelerator Research Complex (J-PARC, Tokai, Japan) at room temperature under dark conditions. Thirty wavelength-shifting fiber-based scintillator neutron detectors with an area of 133 × 133 mm^2 were used to collect the data. A total of 24 data sets were collected using a wavelength of 3.0−5.6 Å with a detector distance of 490 mm. Exposure time for each data set was 9 h at 300 kW. The TOF neutron data were indexed, integrated, scaled, and processed with STARGazer.[22] This large crystal was used for the subsequent X-ray diffraction experiment at room temperature.

2.3. X-ray Diffraction Experiment. X-ray diffraction data from the same crystal as that used for neutron crystallography were collected using an ADSC Quantum270 CCD detector at NE3A in the Photon Factory Advanced Ring (PF-AR; Tsukuba, Japan) at room temperature. The wavelength of the synchrotron radiation, transmittance, and slit size were 1.0 Å, 10%, and 0.05 mm (vertical) × 0.05 mm (horizontal), respectively. The sample-to-detector distance and oscillation range were 150.7 mm and 1.0°, respectively. In an effort to minimize the amount of damage due to radiation, the position of the crystal during irradiation was changed for each shot.[23] A total of 540 images were collected. Data were integrated, merged, and processed with HKL-2000 software.[24] The neutron and X-ray diffraction data statistics are listed in Table 1.

2.4. Structure Refinement. The structure was determined using the "cryo" wild-type PcyA-BV complex structure (PDB ID: 2D1E)[7] from which the water and BV were removed as the initial model. The first refinement was performed using the rigid-body refinement program of CNS[25] with only X-ray diffraction data taken at room temperature from an 8.0−3.0 Å resolution range. The R-factor was reduced from 44.0% to 29.0%. Then, joint refinement was performed with both the neutron and X-ray diffraction data using PHENIX.[26] The 1.95 Å resolution neutron data cut above 1 σ and the 1.55 Å resolution X-ray data were used for structure refinement. Five percent of the data were selected by PHENIX for cross-validation. The neutron-scattering length density and electron density were visualized and manual model refinement was performed using COOT.[27] The geometrical parameters for the BV moiety, hydrogens, and deuteriums were generated by the phenix.ready_set program of PHENIX. The protonation (deuteronation) states of amino acid residues and orientation of the waters were manually adjusted by watching both the neutron-scattering length density and electron density calculated before including hydrogen/deuterium on COOT; only neutron-scattering length density appeared for the positions of the hydrogen (negative density)/deuterium (positive density) atoms. The temperature factors for all atoms and occupancies for hydrogen/deuterium atoms and residues having dual conformations were also refined. During refinements, differences were observed in the conformation of Glu76 between the neutron-scattering length density and X-ray electron density (Supporting Information section 2, Figure S1A). Therefore, we fitted the Glu76 side chain to the neutron-scattering length density and refined the structure to construct the neutron structure of the PcyA-BV complex, which was not markedly affected by X-ray-induced photoreduction (see Results and Discussion). The refinement statistics are listed in Table 2. Figures 3A, 4, 5A, 6, and 8 were produced using PyMOL.[28] The atomic coordinates and structure factors for the neutron structure of the PcyA-BV complex at room temperature (PDB code, 4QCD) have been deposited at the Protein Data Bank (http://www.rcsb.org/). The errors of occupancies of the

DOI: 10.1021/jacs.5b00645
J. Am. Chem. Soc. 2015, 137, 5452−5460

Table 2. Statistics for Structure Refinement

joint refinement		
PDB code	4QCD	
methods	neutron	X-ray
resolution range (Å)	21.2−1.95	36.7−1.55
R_{cryst} [a]	0.167	0.142
R_{free} [b]	0.226	0.165
rms bond angles (deg)	1.38	
rms bond lengths (Å)	0.011	
no. of C atoms	1,337	
no. of N atoms	341	
no. of O atoms	569	
no. of deuterium atoms	760	
no. of hydrogen atoms	2,075	
Ramachandran plot		
most favored (%)	95.2	
additional allowed (%)	4.8	

[a] $R_{cryst} = \Sigma||F_{obs}(hkl)| - |F_{calc}(hkl)||/\Sigma|F_{obs}(hkl)|$. [b] R_{free} is the R_{cryst} calculated for the 5% of the data not included in the refinement.

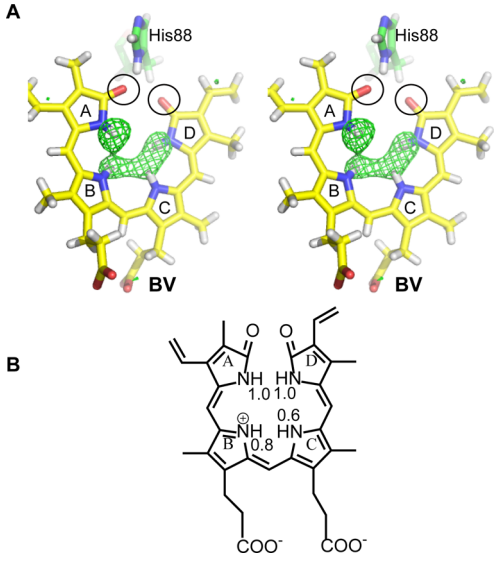

Figure 3. Protonation states of BV. (A) Stereo view of the $F_o - F_c$ neutron-scattering length density omit map (green cage) around the substrate BV at a 3.5 σ contoured level and the structural model. In the calculation, the deuterium and hydrogen atoms of the BV pyrrole rings were omitted from the final model. No residual densities were observed near the lactam (C═O) groups, indicating that no lactim (C−OH) groups were present (black circles). (B) Calculated original occupancies of hydrogens (deuteriums) bound to the four BV pyrrole N atoms considering that all the deuteriums on the BV pyrroles were originally hydrogens.

deuteriums on the pyrrole nitrogens of the BV B- and C-rings were estimated as follows. We constructed 20 models with different occupancies (0.1−1.0; every 0.1 Å^2 for each deuterium), based on the final structure. Then these models were refined with fixed B-factors because the B-factor and occupancy of an individual atom correlate with each other. After refinement, the occupancies for the target deuteriums were compared.

3. RESULTS

3.1. Overall Neutron Structure of the PcyA-BV Complex at Room Temperature. The neutron structure of the PcyA-BV complex at room temperature was refined to a 1.95 Å resolution when diffraction data above 1 σ were used.

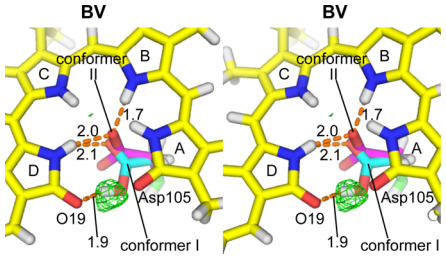

Figure 4. Protonation states of Asp105. Stereo view of the $F_o - F_c$ neutron-scattering length density omit map (green) around Asp105 at a 3.0 σ contoured level and the structural model. The carbon atoms of Asp105 conformer I are colored cyan and those of Asp105 conformer II are colored magenta. The dashed lines represent hydrogen bonds, and the nearby numbers are distances (Å units).

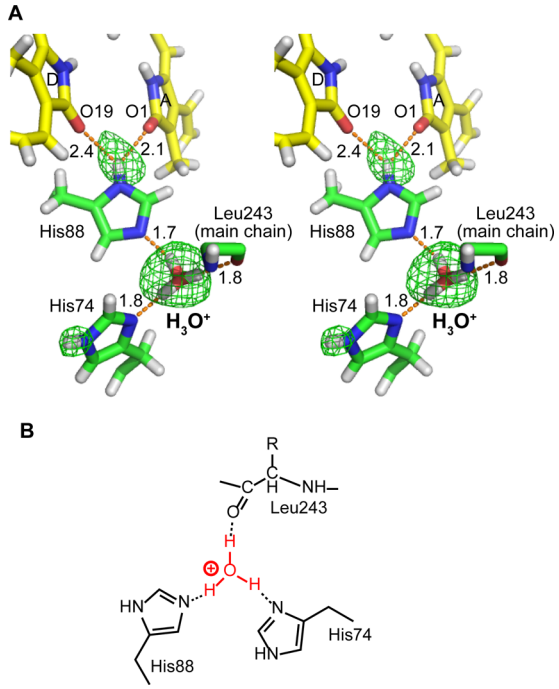

Figure 5. Protonation states of His88 and His74 and the nearby hydronium ion. (A) Stereo view of the $F_o - F_c$ neutron (green cage) omit maps around His74, His88, and the intervening hydronium ion (H_3O^+; actually D_3O^+) at a 3.5 σ contoured level and the structural model. In the calculation, D_3O^+ and the hydrogen/deuterium atoms on the His74 and His88 side chain N atoms were omitted. Hydrogen, oxygen, and nitrogen atoms are colored gray, red, and blue, respectively. The carbon atoms of BV and those of the PcyA enzyme are colored yellow and green, respectively. The dashed lines indicate hydrogen bonds. The numbers indicate distances in Å. To show the hydronium ion clearly, the Leu243 side chain was omitted from the figure. (B) Chemical structure of (A).

The *R*-factor and free *R*-factor were 16.7% and 22.6%, respectively. A total of 2,835 hydrogen/deuterium atoms and 188 hydrating water positions were identified. The overall structure was nearly identical to the "cryo" X-ray structure of the wild-type PcyA-BV complex (PDB ID: 2D1E), with a root-mean-square deviation of the Cα atoms of 0.23 Å when residues 11−240 were superimposed with least-squares fitting. One notable difference between the neutron and X-ray structures was that Glu76, a key residue in PcyA catalysis, was in dual conformations and formed an unfavorable close contact (<2.6 Å) with the exovinyl group of the BV D-ring in

DOI: 10.1021/jacs.5b00645
J. Am. Chem. Soc. 2015, 137, 5452−5460

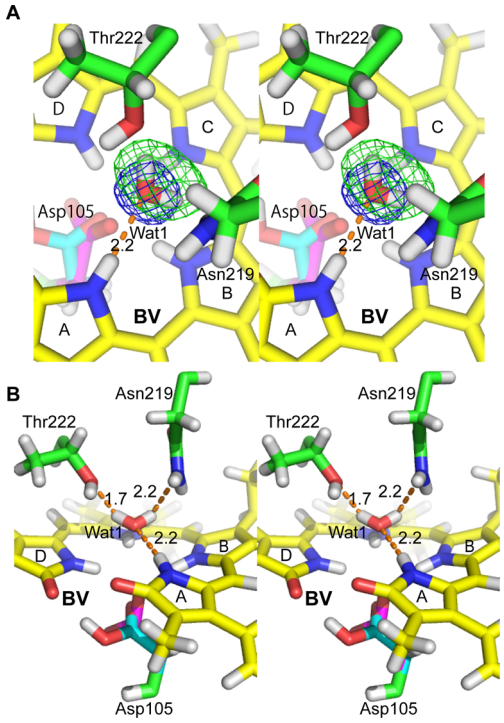

Figure 6. "Axial" water molecule hydrogen bonded to the A-ring pyrrole NH. (A) Stereo view of $F_o - F_c$ neutron (green cage) and electron (blue cage) omit maps, and the structural model around the "axial" water (Wat1) at 4.0 σ and 5.5 σ contoured levels, respectively. The calculation was performed by omitting Wat1 from the final model. The number near the dashed line is the distance in Å. (B) Stereo view of the hydrogen-bonding interaction between Wat1 and Asn219 and Thr222. Dashed lines represent hydrogen bonds. The numbers close to these lines are distances in Å.

the cryo X-ray structure,[7] whereas it was in a single conformation in the neutron structure at room temperature. In the neutron structure, the distance between Glu76 and the BV D-ring exovinyl group was within the normal range (see below). This difference is probably due to X-ray-induced photoreduction during X-ray data collection even under cryo conditions, since, after X-ray irradiation, the crystal exhibited spectroscopic features different from those of the PcyA-BV complex (Supporting Information section 2 and Figure S1). X-rays generate electrons in protein crystals;[29] thus, reduction or side reactions can occur (discussed below). This neutron structure is the first PcyA-BV structure determined at room temperature with a much smaller influence of irradiation than structures obtained by X-ray crystallography (Supporting Information section 1). Other small differences between the previous cryo X-ray structure[7] and this neutron structure are described in Supporting Information section 2.

3.2. Protonation States of Biliverdin IXα. To identify the locations of the hydrogen atoms of BV/BVH$^+$, we generated an $F_o - F_c$ neutron difference Fourier map. The map clearly showed that all of the pyrrole N atoms of BV were deuterated (Figure 3A and Supporting Information Figure S2 and Video S1). All the deuteriums on the BV pyrroles can be considered as originally being hydrogens. Further structural refinement after adding deuterium atoms at these sites revealed that the net occupancies of the deuterium atoms were different among the four pyrrole rings (A–D). The occupancies were calculated to be 1.0, 0.8, 0.6, and 1.0 for the pyrrole-N-bound deuterium atoms of the A-, B-, C-, and D-rings, respectively (Figure 3B). The errors of the occupancies of deuteriums on the pyrrole nitrogens on the BV B- and D-rings were estimated as ±0.05 on the outside. The occupancies of the deuterium atoms on the A- and D-ring pyrroles of BV were 1.0, despite the deuterium atom on the D-ring forming a hydrogen bond with Asp105 (see below). This indicates that the hydrogen–deuterium exchange was complete after soaking the crystals in a deuterated solution. The net deuterium occupancy on the B-ring plus that on the C-ring was 1.4, significantly larger than 1.0, indicating the existence of BV species in which all of the four pyrrole N atoms are deuterated. By contrast, the $F_o - F_c$ neutron difference Fourier map did not show any residual neutron-scattering length density around the lactam (C═O) O atoms (Figure 3A). Therefore, we concluded that there are no lactim (C–OH) forms in BV/BVH$^+$ (i.e., a bis-lactam form).

3.3. Protonation States of Asp105. Asp105 showed dual conformations in the neutron structure similar to those observed in the cryo X-ray structure.[7] Before adding the deuterium atom, there was a region of residual positive $F_o - F_c$ neutron-scattering length density close to the Oδ of one (conformer I) of the two conformers of Asp105 (Figure 4). This is most likely to be a deuterium atom, which forms a hydrogen bond with a lactam O atom (O19) of the BV D-ring. The distance between the Asp105 carboxyl H and O19 was 1.9 Å, and the occupancy of conformer I of Asp105 was refined to be 0.6. The deuterium on the D-ring pyrrole N formed a hydrogen bond with Oδ of the Asp105 conformer I with a distance of 2.1 Å between them (Figure 4). The other conformer (conformer II) of Asp105 was not protonated. One Oδ atom of Asp105 of conformer II appeared to be able to form hydrogen bonds with all of the deuterium atoms on the four pyrrole N atoms. Since the closest atom is the hydrogen on the B-ring pyrrole N (~1.7 Å), and the second is that on the D-ring pyrrole N (2.0 Å), Asp105 (conformer II) probably forms hydrogen bonds with the B-ring and D-ring pyrroles. The other Oδ of Asp105 (conformer II) does not interact with any atom (Figure 4). These results indicate that at least two species of BV (neutral BV and N-protonated BVH$^+$) exist and that Asp105 is complementary to the tautomeric structures of BV.[14]

3.4. Protonation States of His88, His74, and the Newly Identified Intervening Hydronium Ion. His88, as well as Asp105, is an essential residue for PcyA catalysis.[15] This residue is located close to both of the lactam O atoms of BV and should be a proton donor for these groups. The $F_o - F_c$ neutron-scattering length map clearly showed that His88Nδ is protonated (Figure 5A). The residual neutron-scattering length density observed in the vicinity of His88Nε could be favorably interpreted as a deuterium, although it was slightly far from the ideal position and out of the imidazole plane of His88 (Supporting Information section 3 and Figure S3). We carefully reinterpreted the residual density as the deuteron of the nearby water molecule (see below).[14] From the shape of the $F_o - F_c$ neutron-scattering length density map (a symmetric flattened triangular pyramid form), the water appears to exist as a hydronium ion (H_3O^+, actually D_3O^+) (Figure 5A). When we model D_3O^+ at this site, residual density is absent. The three deuterium atoms in D_3O^+ have comparable B-factors (~27–31 Å^2) with occupancies of 1.0. Furthermore, this interpretation produces a protonation state of His88 consistent with the results of an NMR experiment in which His88 was reported as singly protonated.[14] The distance between His88NδH and the lactam O (O1) of the BV A-ring was 2.1 Å, and that of the BV

DOI: 10.1021/jacs.5b00645
J. Am. Chem. Soc. 2015, 137, 5452–5460

D-ring (O19) was 2.4 Å (Figure 5A). Considering that His88 is tilted slightly toward the A-ring of BV, it is likely that the proton is transferred to O1 from His88 during the first reaction step.

His74, which is close to His88, is also a key residue for catalysis; this residue is thought to be involved in a proton relay system.[14] The D_3O^+ close to His88, which was hydrogen bonded to His74, had been interpreted as a water molecule to date. The water was thought to be a proton donor for His88.[10] The $F_o - F_c$ neutron map clearly shows that His74Nε is protonated, whereas His74Nδ is not protonated (Figure 5A). A hydrogen atom of the hydronium ion is hydrogen bonded to the His74Nδ at a distance of 1.8 Å, implying that His74 is not a proton donor for His88 at this stage. As suggested by Kabasakal et al., His74 is likely to be important for forming a hydrogen bond to maintain the hydronium ion with His88 at the active site rather than acting as a proton donor.[10] The remaining hydrogen atoms of the hydronium ion are hydrogen bonded to the main chain carbonyl O atom of Leu243 and Nε of the His88 side chain (Figure 5B). The distances of these hydrogen bonds were 1.8 and 1.7 Å, respectively (Figure 5A).

One additional possible interpretation for the neutron-scattering length density is that the heavy water molecule exists in three conformations (Supporting Information Figure S3C). This moderate resolution neutron-scattering length density map cannot distinguish between D_3O^+ and three partially occupied D_2O molecules; however, if the three D_2O molecules were modeled, His88 and His74 cannot be favorably connected with a hydrogen bond by a D_2O after PHENIX refinements.[26] This structure is not consistent with the earlier mutational study, in which His74 mutation resulted in PcyA-BV complex flexibility.[10] Furthermore, the $F_o - F_c$ neutron-scattering length density map remained between His88 and three D_2Os as a result of the low occupancy of D_2O (average, 0.33) for deuterium atoms (Supporting Information Figure S3C). From these observations, the neutron-scattering length density between His88 and His74 is most probably a D_3O^+.

3.5. Existence of the "Axial" Water Molecule in the Wild-Type PcyA-BV Complex. A peak of $F_o - F_c$ neutron-scattering length density was observed in the vicinity of BV (Figure 6A). Since it was at a position corresponding to the "axial" water molecule found in the structures of the H88Q and D105N mutants,[14] this density was interpreted as the water molecule; however, the water molecule was not identified in a previous cryo X-ray structure of the PcyA-BV complex.[7] We hypothesized that the low level of the corresponding electron density at this site in the previous work was due to X-ray irradiation in the diffraction experiment because high-dose synchrotron X-ray radiation can reduce the active site of redox enzymes even at cryo temperatures.[17] Indeed, the disappearance of the water molecule was experimentally verified in a structural analysis of the H88Q and D105N mutants when the crystals were reduced by sodium dithionite.[14]

Combined with results from the high- and low-dose X-ray irradiation experiments described in Supporting Information section 4, we concluded that the $F_o - F_c$ neutron-scattering length density close to BV (Figure 6A) was derived from a heavy water molecule (assigned as Wat1). The occupancy of Wat1 was 0.5 when only neutron diffraction data were used in the refinement. Two deuterium atom positions for Wat1 were assigned by taking into account the location of the O atom derived from the low electron density (Figure 6A). The deuterium atoms of Wat1 were hydrogen bonded to Thr222 OH and the amide group of the Asn219 side chain (Figure 6B). On the basis of its orientation, Wat1 likely forms a hydrogen bond with the pyrrole NH of the BV A-ring, although the closest pyrrole NH is that of the C-ring. The distance between the O atom of Wat1 and the deuterium atom of the pyrrole A is 2.2 Å (Figure 6A), whereas that of the pyrrole C is 1.7 Å. Since the deuterium atom of the pyrrole C has the lowest occupancy (0.6) among the four deuterium atoms on the four pyrrole rings of BV (Figure 3B), and considering the orientation of Wat1, Wat1 exists at this site when the N atom of the C-ring pyrrole is deprotonated. In other words, Wat1 does not exist when the active site is in the BVH^+/deprotonated Asp105 state because of the ~50% occupancy of Wat1 (Figure 7).

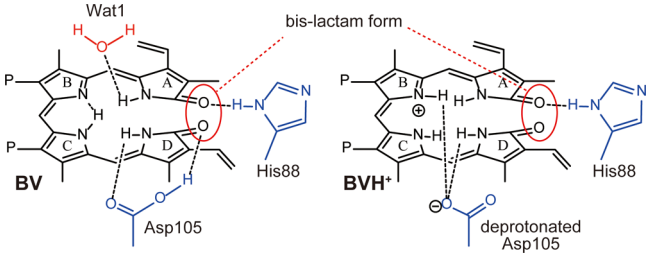

Figure 7. Chemical structures of the two states of BV and the surrounding residues including hydrogens. Neutral BV/Asp105 with Wat1 (left) and BVH^+/deprotonated Asp105 (right). The bis-lactam structures are indicated in red circles.

3.6. Glu76 and the D-Ring Vinyl Group of BV. Glu76 is a vital residue that has been proposed to donate the first proton to BV in the four-electron reduction.[6,12] In the cryo X-ray structure of the wild-type PcyA-BV complex, Glu76 is located in the vicinity of the D-ring vinyl group of BV.[7] Interestingly, this residue exhibited dual conformations, and the distance between Glu76 and the D-ring vinyl group of BV was abnormally short, in a previous cryo X-ray structure.[7] In the neutron structure of the PcyA-BV complex at room temperature, however, the neutron-scattering length density for Glu76 was rather low, and Glu76 was modeled in a single conformation (Figure 8). In addition, the distances between Oε1 and $C18^2$ of BV and that between Oε2 and $C18^1$ of BV were 2.9 and 2.7 Å, respectively, which are within a normal range (Figure 8A). The average bond-length error was calculated as 0.24 Å based on the diffraction precision index (DPI).[30−32] The shape of the neutron-scattering length density for the Glu76 side chain was stubby, implying that Glu76 is rotating or vibrating around the average position. As a result of this side-chain flexibility, the deuterium on the carboxyl group of Glu76 was not identified regardless of the presence of a hydrogen atom. Instead, we observed low $F_o - F_c$ neutron-scattering length density on the 18^1 C of the D-ring vinyl group (Figure 8B). This residual density corresponds to a deuterium atom delivered from Glu76 because the electron density does not appear at the same position in the room temperature X-ray structure. This implies that some BVH^+ in the crystal may have already accepted an electron and a proton (actually deuteron) at this stage for any number of reasons (e.g., reduction by a small amount of prompt γ-rays from NaCl and neutron interactions; see Supporting Information section 1). This is likely consistent with the hypothesis that Glu76 is the initial proton donor.

The discrepancy between the Glu76 conformation described herein and that of the previous cryo X-ray structure is probably

DOI: 10.1021/jacs.5b00645
J. Am. Chem. Soc. 2015, 137, 5452−5460

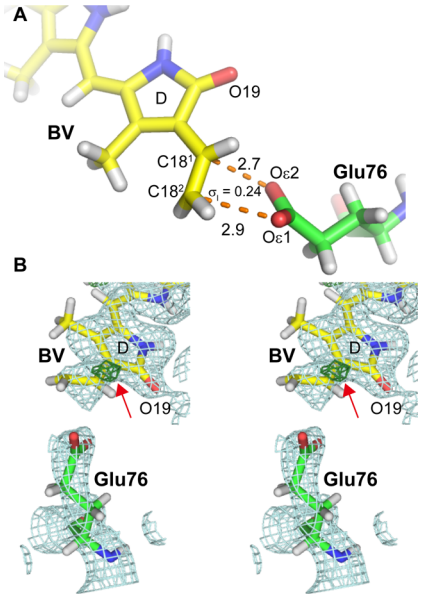

Figure 8. Interaction between Glu76 and the BV D-ring exovinyl group. (A) Close-up view of Glu76 and BV. The numbers near the dashed lines indicate the distances between BV C atoms and the Glu76 carboxyl O atoms (Å units). σ_l indicates the bond-length error value calculated based on the DPI. (B) Stereo view of the BV and Glu76 interaction site. The $2F_o - F_c$ (light blue) and $F_o - F_c$ (dark green) neutron-scattering length density omit maps around BV and Glu76 at 1.5 and 3.5 σ contoured levels and the structural model. The carbon atoms of BV and Glu76 are colored yellow and green, respectively. Hydrogen, oxygen, and nitrogen atoms are colored gray, red, and blue, respectively. The red arrow is to emphasize the position of $F_o - F_c$ neutron-scattering length density. As described above, hydrogens of most C−H groups were not replaced by deuteriums. Since the neutron-scattering length for hydrogen atoms is negative, hydrogens on methylene and methyl groups whose hydrogens were not replaced by deuteriums seem to have no density in the positive $2F_o - F_c$ neutron-scattering length density map.

again due to X-ray-induced photoreduction. We found that Glu76 in the room temperature X-ray structure of PcyA-BV, which was obtained from the same crystal from which the room temperature neutron structure was obtained, approached and was connected to the BV D-ring vinyl group (Supporting Information section 2 and Figure S1). This is an artifact generated by the X-ray irradiation-induced nonenzymatic side reaction. In addition, we observed $F_o - F_c$ X-ray electron density around the D-ring vinyl group and Glu76, which appeared different from the neutron-scattering length density map. These densities suggest that X-ray irradiation also caused the reduction of BV. From these results, we believe that the previous cryo X-ray structure of PcyA-BV[7] may be a combination of the intact damage-free structure, the "enzymatically" reduced structure, and/or the "artificial" reduced structure (Supporting Information Figure S1), which was trapped by the cryo temperature.

4. DISCUSSION

To obtain a high-resolution neutron structure, hydrogen atoms in the PcyA-BV crystal were replaced with deuterium atoms, although most of the hydrogen atoms in the C−H bonds were not replaced. The exchangeable hydrogen atoms must actually be deuterium atoms, although hereafter we use the terms hydrogen, hydronium ion, water, and proton instead of deuterium, D_3O^+, heavy water, and deuteron to discuss the reaction mechanism.

The neutron structure of the PcyA-BV complex suggests that it contains BV in two potential protonation states (Figure 7). In one, hydrogen atoms are bound to three BV pyrroles (neutral BV). In this state, Asp105 is protonated to a neutral state and the axial water (Wat1) exists in the vicinity of BV. In the other state, the four pyrrole N atoms of BV are protonated (N-protonated BVH^+) and Asp105 is deprotonated. In this state, Wat1 does not exist in the vicinity of BV, according to the position of the C-ring pyrrole NH and the orientation of Wat1. Unfortunately, the protonation state of Glu76 was not clearly determined because this residue was flexible at room temperature. Mutational studies and previous high-resolution X-ray structures determined for wild-type and mutant PcyA at cryo temperatures strongly suggest that Glu76 is a proton donor for the exovinyl group of BV.[6,7,12] Indeed, Glu76 was distant from the reduced ethyl group of 18EtBV, the reaction intermediate (Figure 1).[6] Also, we found that a quite low $F_o - F_c$ neutron-scattering length density appeared above the $C18^1$ atom of BV and near to Glu76 (Figure 8B). This implies that, in this neutron structure, an electron and the initial proton have already been delivered to the $C18^1$ atom of BV in some molecules of the crystal. Glu76, the nearest residue to the $C18^1$ atom of BV, is a prime candidate for the proton donor.

In addition, the present neutron analysis of wild-type PcyA clearly indicates that neutral BV and BVH^+ are both in the bis-lactam form (Figures 3 and 7), although a high-field EPR study using the D105N PcyA mutant and Fd suggests that one-electron-reduced BV is in the bis-lactim form.[11] His88 is likely to be a proton donor for the lactam O atom of the BV A-ring (Figures 5 and 7). The Nε of His74 is protonated, whereas its Nδ is deprotonated and is hydrogen bonded to a hydrogen atom of a hydronium ion that is further hydrogen bonded to His88 (Figure 5). Considering the protonation state, His74 is likely to play a role in stabilizing the His88 conformation, as proposed recently.[10] To our knowledge, this work is only the third example to find a hydronium ion in a protein macromolecule.[33,34]

From this study, we provide new information to help understand the catalytic mechanism by which PcyA generates the intermediate 18EtBV from BV on the basis of the bis-lactam form of BV (Figure 9). In substrate-free PcyA, His88 and Asp105 form a hydrogen bond.[8] When PcyA binds BV, this hydrogen bond is broken. The neutron structure of the PcyA-BV complex revealed in the present work is composed of both the neutral BV/Asp105 state and BVH^+/deprotonated Asp105 state, implying that the H^+ that forms BVH^+ is mainly supplied by Asp105. The positively charged BVH^+/deprotonated Asp105 state facilitates electron acceptance. Thereafter, the initial electron generates the neutral BVH radical.[12,13] This intermediate species exists in several equilibrium states involving lactam−lactim alternations. The first proton is transferred from Glu76 to the exovinyl group of the BV D-ring, concomitant with the second electron transfer. The second proton is then transferred via a hydrogen bond from His88Nδ to the lactam O1 of the A-ring to generate a lactim state. Concomitantly, a proton is delivered to His88 from the nearby hydronium ion to keep His88 neutral. A proton is then transferred from the lactim O1 to the lactam O19 of the D-ring. The lactim O19 (OH) of the D-ring attacks the $C18^1$ atom to produce an ethyl group at the D-ring to form 18EtBV. During the reaction to generate 18EtBV from BV, Asp105 likely

DOI: 10.1021/jacs.5b00645
J. Am. Chem. Soc. 2015, 137, 5452−5460

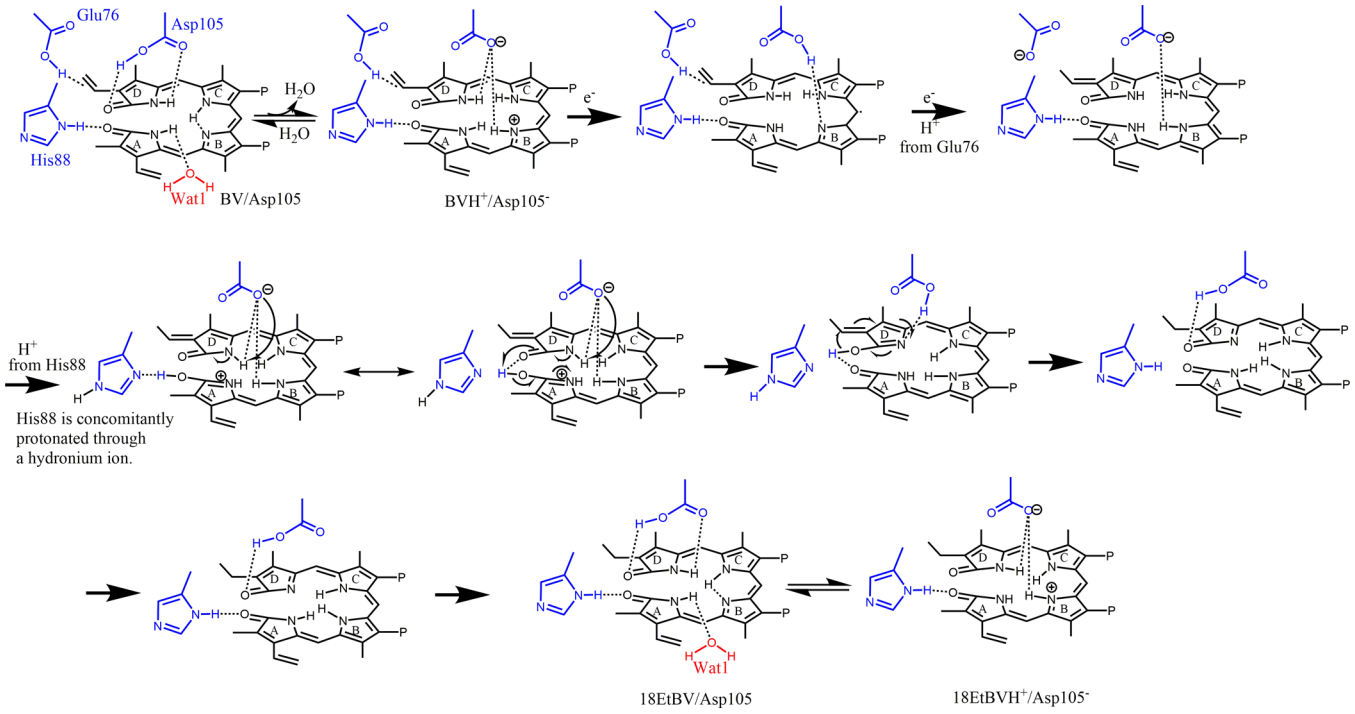

Figure 9. Revised catalytic mechanism for wild-type PcyA to generate 18EtBV from BV based on the neutron structure. See Discussion for details.

mediates proton and electron transfer between itself and BV. The two conformers and flexibility of Asp105 seem to reflect the role of this proton delivery. This mechanism is not inconsistent with results indicating that the D105N PcyA has residual activity,[15] if the nearby water in the D105N PcyA mutant donates the proton, as does Asp105 of wild-type PcyA.

The pH dependence of the catalytic activity was unexpectedly low in acidic conditions (Supporting Information section 5). This may be explained by the observation that the protons on the candidate proton donor(s), Glu76, His88, or Asp105, can be difficult to release under acidic conditions. Considering the pK_a, His88 is likely to be most affected.

Further studies are required to elucidate the full catalytic mechanism of PcyA, for instance, which protons are actually transferred from PcyA to BV, whether 18EtBV is in a bis-lactam state or not, and whether the axial water is in a position and orientation suitable for the protonation of the endovinyl group on the BV A-ring. Such studies include neutron crystallographic analyses of the PcyA-18EtBV complex and/or that of mutants in combination with vibrational spectroscopy and theoretical calculations.

In conclusion, we succeeded in visualizing the detailed structure of PcyA, inclusive of the protonation states of BV and the surrounding residues including Asp105, His88, and His74, by the use of neutron crystallography. The neutron structure minimizes the influence of radiation-induced reduction and reveals two protonation states of BV (neutral BV and BVH^+) in concert with the protonation states of Asp105 (neutral Asp105 and deprotonated Asp105). We also unambiguously demonstrated the presence of the lactam groups of BV in wild-type PcyA, for the first time. In addition, the analysis identified an "axial" water molecule located close to four pyrrole N atoms of BV in the wild-type PcyA, which may be critical for BV A-ring reduction. This "reduction-free" structure will contribute to our understanding of the early steps of PCB synthesis.

■ ASSOCIATED CONTENT

Supporting Information

Detailed structural differences between the neutron structure at room temperature and the cryo X-ray structure, methods, and statistics for X-ray diffraction experiments including high and low-dose irradiation, the single crystal absorption spectrum after the X-ray diffraction experiment, the pH dependence of reactivity, and movies for additional neutron densities. This material is available free of charge via the Internet at http://pubs.acs.org.

■ AUTHOR INFORMATION

Corresponding Author

*unno19@mx.ibaraki.ac.jp

Notes

The authors declare no competing financial interest.

■ ACKNOWLEDGMENTS

We thank members of iBIX at J-PARC for neutron diffraction data collection. The neutron diffraction experiment was conducted under Proposal 2012PX0011 (Ibaraki Prefecture Project). We thank Dr. Yusuke Yamada and other members of the Structural Biology beamlines of PF and members of BL41XU of SPring-8 for X-ray diffraction data collection including preliminary experiments. The X-ray diffraction experiments in PF were conducted under Proposals 2011G519 and 2013G504. Crystallization under microgravity was attempted in the "Kibo" project of the Japan Aerospace Exploration Agency (JAXA). We are grateful to Professor Takamitsu Kohzuma of Ibaraki University for his support and fruitful discussions regarding crystallization. We also thank Professor Masao Ikeda-Saito's laboratory at Tohoku University for use of the microspectrophotometer. This work was partly supported by JSPS KAKENHIs numbers 24570122, 22770096 (to M.U.), and 23370052 (to K.F., K.W., and M.U.), and

DOI: 10.1021/jacs.5b00645
J. Am. Chem. Soc. 2015, 137, 5452−5460

Innovation Research Promotion Program of Ibaraki Univ. (to M.U. and K.K.).

REFERENCES

(1) Dammeyer, T.; Frankenberg-Dinkel, N. *Photochem. Photobiol. Sci.* **2008**, *7*, 1121−1130.
(2) Frankenberg, N. F.; Lagarias, J. C. In *The Porphyrin Handbook*; Kadish, K. M., Sumith, K. M., Guilard, R., Eds.; Academic Press: San Diego, 2003; Vol. *13*, pp 211−235.
(3) Hughes, J.; Lamparter, T. *Plant Physiol.* **1999**, *121*, 1059−1068.
(4) Frankenberg, N.; Lagarias, J. C. *J. Biol. Chem.* **2003**, *278*, 9219−9226.
(5) Unno, M.; Sugishima, M.; Wada, K.; Fukuyama, K. *Integrating Approach Photofunctional Hybrid Materials for Energy and the Environment*, Akitsu, T., Ed.; Nova Publishers: New York, 2013; pp 47−67.
(6) Hagiwara, Y.; Sugishima, M.; Khawn, H.; Kinoshita, H.; Inomata, K.; Shang, L.; Lagarias, J. C.; Takahashi, Y.; Fukuyama, K. *J. Biol. Chem.* **2010**, *285*, 1000−1007.
(7) Hagiwara, Y.; Sugishima, M.; Takahashi, Y.; Fukuyama, K. *Proc. Natl. Acad. Sci. U. S. A.* **2006**, *103*, 27−32.
(8) Hagiwara, Y.; Sugishima, M.; Takahashi, Y.; Fukuyama, K. *FEBS Lett.* **2006**, *580*, 3823−3228.
(9) Wada, K.; Hagiwara, Y.; Yutani, Y.; Fukuyama, K. *Biochem. Biophys. Res. Commun.* **2010**, *402*, 373−377.
(10) Kabasakal, B. V.; Gae, D. D.; Li, J.; Lagarias, J. C.; Koehl, P.; Fisher, A. J. *Arch. Biochem. Biophys.* **2013**, *537*, 233−242.
(11) Stoll, S.; Gunn, A.; Brynda, M.; Sughrue, W.; Kohler, A. C.; Ozarowski, A.; Fisher, A. J.; Lagarias, J. C.; Britt, R. D. *J. Am. Chem. Soc.* **2009**, *131*, 1986−1995.
(12) Tu, S. L.; Rockwell, N. C.; Lagarias, J. C.; Fisher, A. J. *Biochemistry* **2007**, *46*, 1484−1494.
(13) Tu, S. L.; Gunn, A.; Toney, M. D.; Britt, R. D.; Lagarias, J. C. *J. Am. Chem. Soc.* **2004**, *126*, 8682−8693.
(14) Kohler, A. C.; Gae, D. D.; Richley, M. A.; Stoll, S.; Gunn, A.; Lim, S.; Martin, S. S.; Doukov, T. I.; Britt, R. D.; Ames, J. B.; Lagarias, J. C.; Fisher, A. J. *Biochemistry* **2010**, *49*, 6206−6218.
(15) Tu, S. L.; Sughrue, W.; Britt, R. D.; Lagarias, J. C. *J. Biol. Chem.* **2006**, *281*, 3127−3136.
(16) Chance, B.; Angiolillo, P.; Yang, E. K.; Powers, L. *FEBS lett* **1980**, *112*, 178−182.
(17) Berglund, G. I.; Carlsson, G. H.; Smith, A. T.; Szoke, H.; Henriksen, A.; Hajdu, J. *Nature* **2002**, *417*, 463−468.
(18) Wuerges, J.; Lee, J. W.; Yim, Y. I.; Yim, H. S.; Kang, S. O.; Djinovic Carugo, K. *Proc. Natl. Acad. Sci. U. S. A.* **2004**, *101*, 8569−8574.
(19) Niimura, N., Podjarny, A. *Neutron Protein Crystallography: Hydrogen, Protons, and Hydration in Biomacromolecules*; IUCr Monographs on Crystallography 25; Oxford University Press: New York, 2011; pp 1−233.
(20) Tanaka, I.; Kusaka, K.; Hosoya, T.; Niimura, N.; Ohhara, T.; Kurihara, K.; Yamada, T.; Ohnishi, Y.; Tomoyori, K.; Yokoyama, T. *Acta Crystallogr., Sect. D* **2010**, *66*, 1194−1197.
(21) Kusaka, K.; Hosoya, T.; Yamada, T.; Tomoyori, K.; Ohhara, T.; Katagiri, M.; Kurihara, K.; Tanaka, I.; Niimura, N. *J. Synchrotron Radiat.* **2013**, *20*, 994−998.
(22) Ohhara, T.; Kusaka, K.; Hosoya, T.; Kurihara, K.; Tomoyori, K.; Niimura, N.; Tanaka, I.; Suzuki, J.; Nakatani, T.; Otomo, T.; Matsuoka, S.; Tomita, K.; Nishimaki, Y.; Aijima, T.; Ryufuku, S. *Nucl. Instrum. Methods Phys. Res., Sect. A* **2009**, *600*, 195−197.
(23) Zeldin, O. B.; Gerstel, M.; Garman, E. F. *J. Synchrotron Radiat.* **2013**, *20*, 49−57.
(24) Otwinowski, Z.; Minor, W. Processing of X-ray Diffraction Data Collected in Oscillation Mode. In *Methods in Enzymology: Macromolecular Crystallography, Part A*; Carter, C. W., Jr., Sweet, R. M., Eds.; Academic Press: New York, 1997; Vol. *276*, pp 307−326.
(25) Brunger, A. T.; Adams, P. D.; Clore, G. M.; DeLano, W. L.; Gros, P.; Grosse-Kunstleve, R. W.; Jiang, J. S.; Kuszewski, J.; Nilges, M.; Pannu, N. S.; Read, R. J.; Rice, L. M.; Simonson, T.; Warren, G. L. *Acta Crystallogr., Sect. D* **1998**, *54*, 905−921.
(26) Adams, P. D.; Afonine, P. V.; Bunkoczi, G.; Chen, V. B.; Davis, I. W.; Echols, N.; Headd, J. J.; Hung, L. W.; Kapral, G. J.; Grosse-Kunstleve, R. W.; McCoy, A. J.; Moriarty, N. W.; Oeffner, R.; Read, R. J.; Richardson, D. C.; Richardson, J. S.; Terwilliger, T. C.; Zwart, P. H. *Acta Crystallogr., Sect. D* **2010**, *66*, 213−221.
(27) Emsley, P.; Cowtan, K. *Acta Crystallogr., Sect. D* **2004**, *60*, 2126.
(28) DeLano, W. L. *The PyMOL Molecular Graphics System*; DeLano Scientific LLC: Palo Alto, CA, 2002.
(29) Casadei, C. M.; Gumiero, A.; Metcalfe, C. L.; Murphy, E. J.; Basran, J.; Concilio, M. G.; Teixeira, S. C.; Schrader, T. E.; Fielding, A. J.; Ostermann, A.; Blakeley, M. P.; Raven, E. L.; Moody, P. C. *Science* **2014**, *345*, 193−197.
(30) Cruickshank, D. W. *Acta Crystallogr., Sect. D* **1999**, *55*, 583−601.
(31) Blow, D. M. *Acta Crystallogr., Sect. D* **2002**, *58*, 792−797.
(32) Gurusaran, M.; Shankar, M.; Nagarajan, R.; Helliwell, J. R.; Sekar, K. *IUCrJ* **2014**, *1*, 74−81.
(33) Cuypers, M. G.; Mason, S. A.; Blakeley, M. P.; Mitchell, E. P.; Haertlein, M.; Forsyth, V. T. *Angew. Chem., Int. Ed. Engl.* **2013**, *52*, 1022−1025.
(34) Kovalevsky, A. Y.; Hanson, B. L.; Mason, S. A.; Yoshida, T.; Fisher, S. Z.; Mustyakimov, M.; Forsyth, V. T.; Blakeley, M. P.; Keen, D. A.; Langan, P. *Angew. Chem., Int. Ed. Engl.* **2011**, *50*, 7520−7523.

DOI: 10.1021/jacs.5b00645
J. Am. Chem. Soc. 2015, 137, 5452−5460